

## Computational Neuroscience

## Extracellular spike detection from multiple electrode array using novel intelligent filter and ensemble fuzzy decision making

Hamed Azami<sup>a,\*</sup>, Javier Escudero<sup>a</sup>, Ali Darzi<sup>b</sup>, Saeid Sanei<sup>c</sup><sup>a</sup> Institute for Digital Communications, School of Engineering, University of Edinburgh, UK<sup>b</sup> Institute for Research in Fundamental Sciences (IPM), Iran<sup>c</sup> Department of Computing, Faculty of Engineering and Physical Sciences, University of Surrey, UK

## HIGHLIGHTS

- Neuronal data are used in many scientific and clinical applications.
- Spike detection methods are needed to estimate the time instants of action potentials.
- We suggest utilizing a novel approach to choose the filter parameters automatically.
- Hilbert transform is employed as a pre-processing step.
- We propose two novel approaches to combine some existing spike detectors.

## ARTICLE INFO

## Article history:

Received 8 July 2014

Received in revised form 3 October 2014

Accepted 9 October 2014

Available online 18 October 2014

## Keywords:

Extracellular spike detection

Evolutionary algorithms

Hilbert transform

Fuzzy and probability theory

Ensemble empirical mode decomposition

## ABSTRACT

**Background:** The information obtained from signal recorded with extracellular electrodes is essential in many research fields with scientific and clinical applications. These signals are usually considered as a point process and a spike detection method is needed to estimate the time instants of action potentials. In order to do so, several steps are taken but they all depend on the results of the first step, which filters the signals. To alleviate the effect of noise, selecting the filter parameters is very time-consuming. In addition, spike detection algorithms are signal dependent and their performance varies significantly when the data change.

**New methods:** We propose two approaches to tackle the two problems above. We employ ensemble empirical mode decomposition (EEMD), which does not require parameter selection, and a novel approach to choose the filter parameters automatically. Then, to boost the efficiency of each of the existing methods, the Hilbert transform is employed as a pre-processing step. To tackle the second problem, two novel approaches, which use the fuzzy and probability theories to combine a number of spike detectors, are employed to achieve higher performance.

**Results, comparison with existing method(s) and conclusions:** The simulation results for realistic synthetic and real neuronal data reveal the improvement of the proposed spike detection techniques over state-of-the-art approaches. We expect these improve subsequent steps like spike sorting.

© 2014 Elsevier B.V. All rights reserved.

## 1. Introduction

Multiple electrode array (MEA) is a usual tool in neuroscience that records simultaneous activity of several neurons in a piece of neural tissue. The electrode may be intracellular, although it is more

commonly extracellular. The recorded signals are small, and they frequently arise from electrical activity in some nearby neurons (Azami and Sanei, 2014; Smith et al., 2007).

The majority of techniques for the analysis of neural activity begin with spike detection to identify the time instants at which action potentials occurred from one or several neurons. The quality of the spike detection algorithm notably influences the performance of the subsequent steps, such as spike sorting (grouping the recorded spikes into clusters based on the similarity of their shapes). Errors in detecting the number and location of spikes will

\* Corresponding author. Tel.: +44(0) 747 7194150.

E-mail addresses: [hamed.azami@ed.ac.uk](mailto:hamed.azami@ed.ac.uk) (H. Azami), [javier.escudero@ed.ac.uk](mailto:javier.escudero@ed.ac.uk) (J. Escudero), [ali.darzi@ipm.ir](mailto:ali.darzi@ipm.ir) (A. Darzi), [s.sanei@surrey.ac.uk](mailto:s.sanei@surrey.ac.uk) (S. Sanei).

inevitably propagate through all later analyses (Azami and Sanei, 2014; Martinez et al., 2009; Nenadic and Burdick, 2005).

There are a number of reasons that make the spike detection a challenging task. First, extracellularly recorded spike trains are unavoidably corrupted by the superimposed activity of multiple neurons and the noise from the recording hardware. Second, implanted microelectrodes usually pick up the concurrent electrical activities with various sizes and shapes from an unknown number of local neurons. Third, the activity of distant neurons may emerge as noise that is highly correlated with the useful signal (Nenadic and Burdick, 2005; Liu et al., 2012).

Few decades ago, spike detection was being performed by using simple amplitude thresholds. This method detects events, like spikes, by considering a peak that is higher than a threshold defined by a user or a statistical property of a signal, such as mean, standard deviation, or median. The threshold can be selected manually by visual inspection or automatically. Although this kind of spike detection method is appropriate for intracellular recordings, extracellular recordings from high-density MEAs and low-impedance microelectrodes frequently have low signal-to-noise ratio (SNR), and the problem becomes far more complex (Kim and McNames, 2007; Maccione et al., 2009).

Another widespread method to detect spikes is based on **template matching**, a technique used in signal and image processing. In this method, templates representing a typical waveform are utilized as benchmarks. The initial stage of this method is to select a waveform that represents a typical spike shape as template. In the second stage, the method locates possible events in the signal that “closely resemble” the template. Finally, there is a thresholding stage. Early template matching methods often started with the experimenter identifying a couple of high-quality spikes, and using them to train a filter. However, this is unfeasible, especially when there are a large number of electrodes (Azami and Sanei, 2014; Kim and McNames, 2007; Shahid et al., 2010). Even though the template matching algorithm often detects spike events better than simple threshold algorithms, its performance depends on a **priori knowledge** of the spike shape to create the template. In addition, since the automatic selection of a template in a noisy neuronal data is very complicated, the performance of the method **decreases in poor SNRs** (Azami and Sanei, 2014; Kim and McNames, 2007; Shahid et al., 2010).

In Liu et al. (2012), an automatic spike detection method based on **piecewise optimal morphological filter** is suggested. The interesting benefit of this method is that the piecewise optimal morphological filter can highlight the spikes categorized by their structural elements and successfully reduce the background noise. However, the method **missed spike events with dissimilar morphological characters** from most of spike events presented in data window. This increased the false detection rate of the algorithm notably. This problem was, at least partially, due to the fact that the burst of one or two types of spikes makes the rest type of spikes uncommon within the data window, which leads to the bias of optimal structuring elements to bursting spikes.

A **model-based algorithm** to detect the spikes by taking into account the distributions of spike amplitudes, widths and frequencies was suggested in Takekawa et al. (2014). Quiroga showed that spike shapes can be distorted significantly by the causal filters frequently used for online spike detection. He illustrated this impact using **elliptic filters**, but similar results were obtained with **Butterworth or Chebyshev causal filters** (Quiroga, 2009).

There are also a number of approaches based on **wavelet transform** to detect the spikes in neuronal data (Nenadic and Burdick, 2005; Yang and Shamma, 1988). In Yang and Shamma (1988), a spike detection method using **discrete Haar transformation**, which does not need a priori assumptions about spike shape or timing, was proposed. However, the approach assumed white noise

and required an unnecessary inverse transformation from wavelet domain to time domain (Nenadic and Burdick, 2005). To overcome this problem, Nenadic and Burdick combined wavelet transforms with basic detection theory to enhance an unsupervised method for detecting spikes in extracellular neural recordings robustly (Nenadic and Burdick, 2005). The most important advantage of this approach is its ability to separate signals from noise by thresholding the wavelet coefficients and, therefore, this method **performs well even in poor SNR**. However, its main disadvantage is the need to assume a single spike shape resulting in the wavelet choice that is suboptimal for other spikes (Shahid et al., 2010).

Another well-known approach uses signal transformations such as nonlinear energy operator (NEO or NLEO). This is a powerful tool for spike detection. However, **when the signal contains multiple frequencies or components, the output of the method includes a DC part and a time-varying part, called cross-terms**. The cross-terms and the presence of noise reduce the accuracy of this spike detection algorithm (Azami and Sanei, 2014; Kim and McNames, 2007; Shahid et al., 2010). To overcome these problems, Azami and Sanei employed **the smoothed NEO (SNEO)** and some filters to detect the spikes in noisy neuronal data (Azami and Sanei, 2014).

Mtewa and Smith have presented five spike detection algorithms and three thresholding criteria for spike detection (Mtewa and Smith, 2006). Among them, the best method was based on normalized cumulative energy difference (NCED). This method, inspired by the fact that **the energy in a spike (either positive or negative) should be greater than that in noise of the same length**, can be followed by **multi-template-based spike sorting**.

In Azami and Sanei (2014), three new methods to detect the neuronal spikes buried in noise and interferences based on SNEO, fractal dimension (FD) and standard deviation were proposed. In order to overcome the impact of noise and to overcome the low speed of discrete wavelet transform (DWT), singular spectrum analysis (SSA), Kalman filter (KF) and **Savitzky–Golay filter** were used as **pre-processing steps**. In addition, since DWT, SSA, KF and Savitzky–Golay filter have several tunable parameters, Azami and Sanei proposed to use the residual signal obtained by empirical mode decomposition (EMD) as a filtered signal (Azami and Sanei, 2014).

To sum up, there are still two outstanding problems in spike detection: (1) usually, **choosing appropriate parameters** for each noise reduction method is a time-consuming task and needs to be done in many trials. (2) Generally, each spike detection approach is only suitable **for a limited number of signal types and applications**.

In order to overcome the first problem, we now propose an intelligent approach to set appropriate filter parameters automatically by two powerful evolutionary algorithms, namely **genetic algorithm (GA)** and **new particle swarm optimization (NPSO)**. In addition, we suggest using **an ensemble EMD (EEMD) method** as a pre-processing noise reduction step. EEMD is a powerful new algorithm to decompose a complex time series into a number of intrinsic mode functions (IMFs) and a residual signal and it achieves better performance than EMD (Mandic et al., 2013). After using an intelligent filter or an EEMD to increase the accuracy of the existing methods, we propose to employ the Hilbert transform (Benitez et al., 2001).

In order to tackle the second problem and achieve much better performance compared with those of the conventional neuronal data spike detection methods, we also propose two approaches based on the probability and fuzzy concepts that combine some existing approaches.

In the following section, the proposed intelligent filter and two methods to combine the existing algorithms are explained. Section 3 provides describes the dataset employed in this paper. Then, the results of the proposed methods and the conventional ones

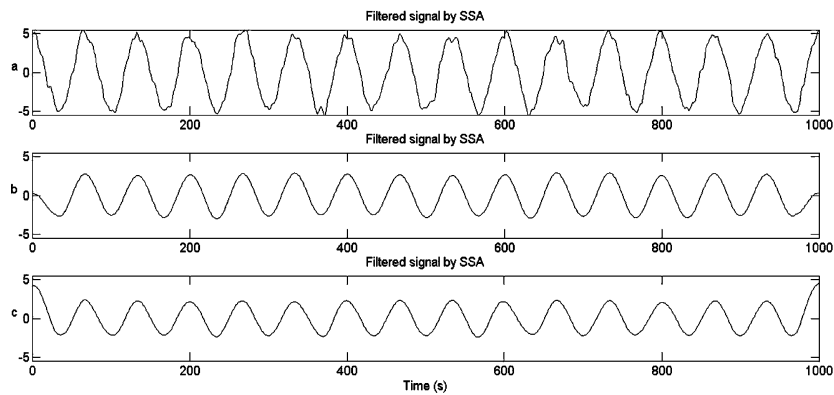


Fig. 1. Results of applying three different sets of  $l$  and  $l$  for the SSA: (a)  $l = 6$  and  $l = [1]$ , (b)  $l = 30$  and  $l = [1]$ , and (c)  $l = 30$  and  $l = [2]$ .

are compared. The conclusions of the paper are stated in the last section.

## 2. Proposed methods

First, we explain a novel approach for selecting parameters automatically as well as introducing EEMD briefly. Then, the importance of using Hilbert transform for this application is described. Finally, two novel methods for extracellular spike detection based on the fuzzy and probability concepts are defined in detail.

### 2.1. Noise reduction methods

In this subsection, we discuss an intelligent filtering approaches and EEMD.

#### 2.1.1. Intelligent approach for filtering

Here, we explain an approach to filter a signal. First, we introduce the SSA briefly and then propose an approach to enhance it. Next, after describing the Savitzky–Golay filter (Azami and Sanei, 2014), we suggest an approach to improve it by the NPSO.

**2.1.1.1. Improved singular spectrum analysis by genetic algorithm.** SSA, which is a flexible and powerful filtering tool suitable for many different types of signals, uses a subspace selection and reconstruction to make a desired signal (Sanei et al., 2012; Azami and Sanei, 2012). It is much faster than many existing filters such as those based on DWT and has been used for spike detection recently (Azami and Sanei, 2014). However, this process, like almost all filters, has an important short-coming, i.e. there are some parameters to be adjusted using a large number of trials. Sometimes, the range or average of the SNR is known or estimated. In this case, we propose a new method based on the GA. GA is a powerful search algorithm to find the approximate solutions in the defined space (Azami et al., 2013).

As a means of illustration, assume a Gaussian noise with  $\text{SNR} = 2$  dB is added to  $x_1 = 5\sin(3\pi t)$ . There are many ways for choosing the two parameters of SSA, i.e. window length (i.e. embedding dimension),  $l$  and  $m$  disjoint subsets  $l = [l_1, \dots, l_m]$  to reconstruct the time series. The filtering process for a particular signal is sensitive to selection of these parameters. When  $l$  and  $l$  are selected too large, some important information of the original signal is removed by this filter. For too small  $l$  and  $l$ , however, this filter cannot attenuate destructive noises sufficiently. Moreover, in many applications due to lack of information about a signal, selecting

these parameters is very difficult. To overcome this problem, in this study, we propose to use the GA with the following fitness function:

$$H = |\text{SNR} - \bar{\text{SNR}}| = \left| 10 \log_{10} \left( \frac{\sum_{i=1}^n (x_f(i))^2}{\sum_{i=1}^n (x(i) - x_f(i))^2} \right) - \bar{\text{SNR}} \right| \quad (1)$$

where  $n$ ,  $x$ ,  $x_f$ , and  $\bar{\text{SNR}}$  are length of the signal, noisy signal, filtered signal, and SNR average of the original signal, respectively.  $x - x_f$  is the noise. In other words, the GA tries to reduce  $H$  by changing  $l$  and  $l$  for the SSA. It should be mentioned that we use the proposed improved filter where the SNR average or at least the range of noise power is known. The GA employed here has 20 populations and the number of iterations is 30.

The results for three different sets of  $l$  and  $l$  are shown in Fig. 1. As can be seen in Fig. 1a,  $l = 6$  and  $l = [1]$ , where  $[k]$  states that only  $k$  eigentriples are used, are not large enough for filtering the signal with an  $\text{SNR} = 2$  dB. In Fig. 1b,  $l = 30$  and  $l = [1]$  and in Fig. 1c,  $l = 30$  and  $l = [2]$  are chosen. It is evident that in both figures the amplitudes decrease considerably for an original signal with amplitude 5. Figs. 1b and c demonstrates irregularities in the first and the last time samples. Here, GA is used to select suitable sets of filter parameters for  $\text{SNR} = 2$  dB. The result of employing the proposed filter is shown in Fig. 2c.

**2.1.1.2. Improved Savitzky–Golay filter by new particle swarm optimization.** The idea of using computational methods to estimate an optimal set of parameters to filter the signals can be generalized for every kind of filter. For example, a powerful, fast, and flexible filter widely used in biomedical signal processing is the Savitzky–Golay filter (Savitzky and Golay, 1964; Lue et al., 2005).

The coefficients of a Savitzky–Golay filter, when applied to a signal, perform a polynomial fitting  $P$  of the degree  $K$  to  $N = N_r + N_l + 1$  points of the signal, where  $N$  is the window size and  $N_r$  and  $N_l$  are signal points in the right and left of a current signal point, respectively. One of the best important advantages of this filter is that it tends to keep the distribution extreme points, which are often flattened by other smoothing techniques (Savitzky and Golay, 1964; Lue et al., 2005). This makes the Savitzky–Golay filter a favorable tool to detect the spikes. However, this filter has the aforementioned short-coming of requiring the adjustment of some parameters using a large number of trials. When  $N$  and  $K$  are selected too large, some important information of the original signal is removed by this filter. For too small  $N$  and  $K$ , however, this filter cannot attenuate destructive noises sufficiently.

Moreover, in many applications, due to the lack of information about the best polynomial order to fit a signal, selecting  $K$  is very difficult. To overcome this problem, in this study, we propose to use NPSO as a powerful and fast evolutionary algorithm (Azami et al., 2014) with a fitness function the same as Eq. (1).

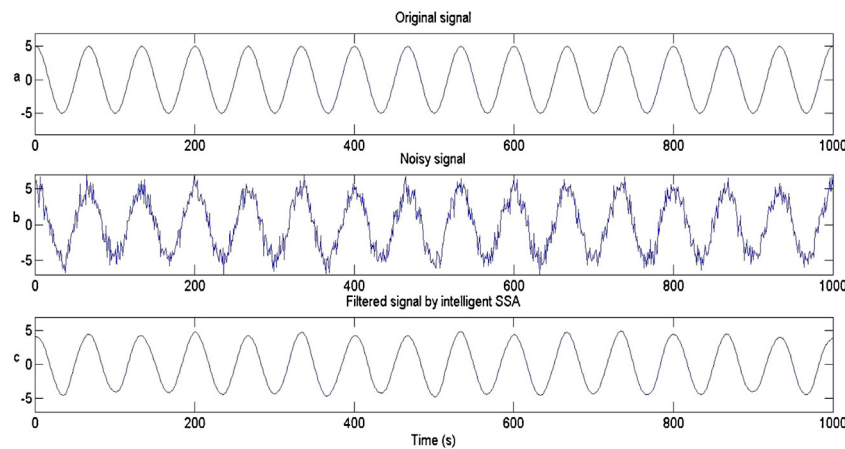


**Fig. 2.** Improved SSA by GA; (a) original signal, (b) noisy signal (SNR = 2 dB), and (c) optimal filtered signal.

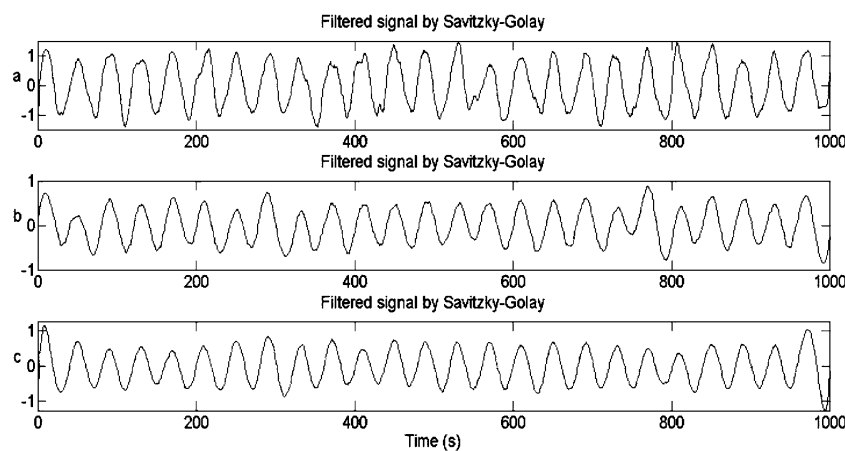


**Fig. 3.** Results of applying three different sets of  $K$  and  $N$  for the Savitzky–Golay filter: (a)  $K=3$  and  $N=19$ , (b)  $K=5$  and  $N=31$ , and (c)  $K=3$  and  $N=61$ .

This is again illustrated using a similar setting to that of SSA. Assume a Gaussian noise with SNR = 5 dB is added to  $x_2 = \sin(5\pi t)$ . The results for three different sets of  $K$  and  $N$  are shown in Fig. 3. As can be seen in Fig. 3a,  $K=3$  and  $N=19$  are not large enough for filtering the signal with an SNR = 5 dB. In Fig. 3b,  $K=5$  and  $N=31$ , and in Fig. 3c  $K=3$  and  $N=61$  are chosen. It is evident that in both figures the amplitudes decrease considerably for an original

signal with amplitude 1. Fig. 3b shows abnormalities in about 280 and 770 samples and Fig. 3c demonstrates irregularities in the first and the last time samples. Here, NPSO is used to select suitable sets of filter parameters primarily for SNR = 5 dB. The result of employing the proposed filter is shown in Fig. 4c. In the proposed approach, the parameters of the NPSO method, as for other evolutionary algorithms, are manually chosen as follows: population

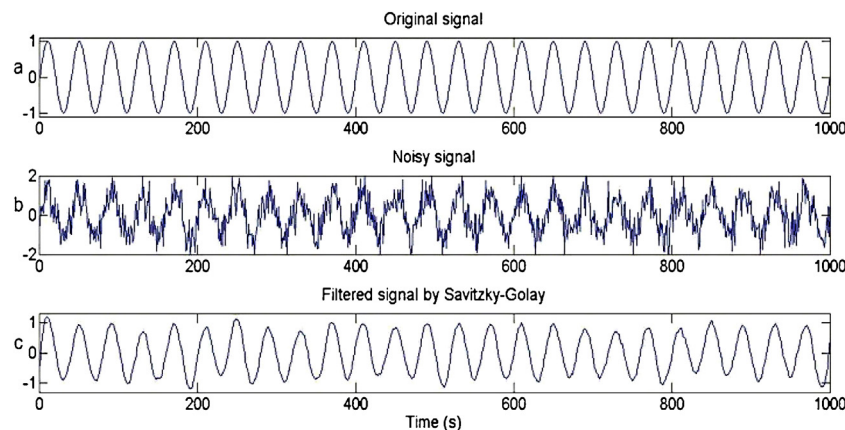


**Fig. 4.** Improved Savitzky–Golay filter by NPSO; (a) original signal, (b) noisy signal (SNR = 5 dB), and (c) optimal filtered signal.



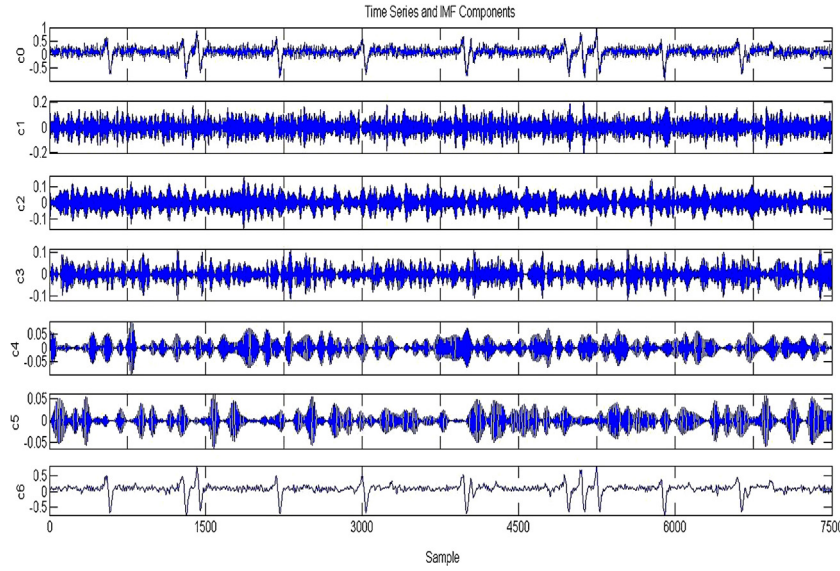


**Fig. 5.** Components of the restored realistic synthetic signal by EEMD. The first time series is the filtered signal. The decomposition yields 5 IMF and a residual. The IMFs are the time-frequency constituents or components of the realistic synthetic neuronal signal.

size = 30;  $C_1 = C_2 = 2$ ; dimension = 2; iteration = 50;  $w = 1$ ;  $2 \leq K \leq 10$ ;  $3 \leq N \leq 201$ . It must be noted, however, that the performance of the NPSO is robust to small deviations from this set of parameters. Finally, note that in this filter,  $K$  must be less than  $N$  and  $N$  must be odd.

### 2.1.2. Ensemble empirical mode decomposition

The use of EMD has been proved to have many advantages in biomedical signal processing (Mandic et al., 2013). However, EMD results may suffer from (1) Mode mixing, whereby either an IMF includes different oscillatory modes, or one mode is in different IMFs; and (2) Aliasing when there are overlapping of IMF spectra caused by a sub-Nyquist nature of extrema sampling (Maccione et al., 2009). Hence, in this paper we propose to employ EEMD, instead of EMD, to reduce the noise.

The EEMD algorithm is explained briefly as follows:

- (1) A white noise signal,  $n_i(t)$ , is added to the signal  $x(t)$ :  $x_i(t) = x(t) + n_i(t)$ ,  $i \in [1, N]$ , with  $N$  suggested to be a few hundreds.
- (2) EMD is performed on each  $x_i(t)$ .
- (3) The ensemble mean of each IMF is taken as the final result (Lin and Li, 2011).

As stated in Azami and Sanei (2014), the residual signal obtained by EEMD can be considered as a filtered version of the signal extracted from an original signal combined with some noise sources with mean values of zero. In Fig. 5, we can see the result of decomposition performed by EEMD of the filtered test signal. This figure illustrates that modes are ordered from highest to lowest frequencies. As mentioned before, the very important advantage of employing EEMD is that unlike more traditional filtering techniques, the EEMD parameters do not need to be adjusted.

### 2.2. Hilbert transform

After applying the noise reduction algorithms and to increase the accuracy of the spike detection methods, we propose to employ the Hilbert transform to enhance the spikes (Thrane et al., 1995). Consider the concept of the analytic signal (also named pre-envelope) of a signal  $x(t)$ . This can be expressed by:

$$y(t) = x(t) + j\hat{x}(t) \quad (2)$$

The envelope  $B(t)$  of  $y(t)$  can be defined as:

$$B(t) = \sqrt{x^2(t) + \hat{x}^2(t)} \quad (3)$$

One of the most important characteristics of the Hilbert transform is that it is an odd function. In other words, it will cross zero on the  $x$ -axis every time that there is an inflexion point in the original waveform. Correspondingly, a crossing of the zero between consecutive positive and negative inflexion points in the original waveform will be demonstrated as a spike in its Hilbert transformed conjugate. This can be seen in Fig. 6. This remarkable characteristic can be used to develop an elegant and much easier way to find the spike of a signal (Benítez et al., 2001; Thrane et al., 1995).

### 2.3. Two hybrid approaches for spike detection

After using Hilbert transform, the literature describes some methods to detect the spikes. They are based on SNEO, KF, standard deviation, and matching algorithms. Each of them has its advantages and disadvantages. We propose two techniques to combine some of the conventional methods. These proposed techniques are based on the fuzzy and probability concepts to increase the accuracy of spike detection approaches. For each sample, we consider:

$$HC = \frac{\lambda_1 SDA_1 + \lambda_2 SDA_2 + \dots + \lambda_n SDA_n}{SDA_1 + SDA_2 + \dots + SDA_n} \quad (4)$$

where if the spike of the  $i$ th spike detection method is detected  $\lambda_i = 1$  else  $\lambda_i = 0$ .  $n$  is the number of considered spike detection methods and  $SDA_i$  is spike detection accuracy of  $i$ th considered method by using semi-real data. In fact, this technique is originated from the concept of existence or absence probability of a sample as a spike. Thus, if this probability is more than 0.5 we assume this signal sample is indeed a spike and vice versa. As it is clear, for semi-real data if  $SDA_m$  is larger than  $SDA_n$ ,  $m$ th method is more reliable and trustworthy than  $n$ th method, so we show this effect on Eq. (5).

Two different parameters, namely, the true positive (TP) and false positive (FP) ratios were used to evaluate the performance of the proposed and conventional methods. These parameters are defined as  $TP = (N_t/N)$  and  $FP = (N_f/N)$ ; where  $N_t$ , and  $N_f$  respectively represent the number of correctly and falsely detected spikes and  $N$  shows the actual number of spikes. It should be mentioned, since the false negative (FN) parameter used to assess the spike detection

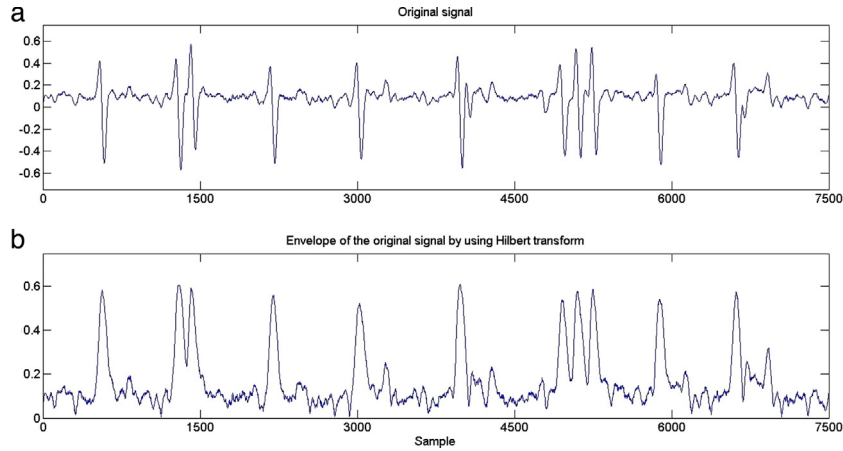


**Fig. 6.** The original signal (a) and the signal after the proposed Hilbert transform was applied (b).

methods is dependent on TP ( $TP = 1 - FN$ ), in this paper we only consider TP and FP ratios. Considering that FP is based on the inability to detect spikes, we define  $SDA = (TP + (1 - FP)/2)$ . It is worth noting that TP ratio is known as sensitivity too (Procházka et al., 2014).

As an example, we consider a part of a real signal of the CARMEN project managed by Prof. Leslie S. Smith (CARMEN, 2014). This part of the signal is shown in Fig. 7a. Some spike detection approaches for semi-real neuronal data were presented in Azami and Sanei (2014). We now combine five of these methods to assess the real neuronal signal. Based on the SDAs of those methods provided in Table 1 in Azami and Sanei (2014) and on the fact that the real signal has about SNR equals to 0 dB, by replacing TP and FP values in the above equation we have  $SDA_1 = 0.9$ ,  $SDA_2 = 0.87$ ,  $SDA_3 = 0.83$ ,  $SDA_4 = 0.89$ , and  $SDA_5 = 0.86$ .

Hence, for the first line we have  $HC(1) = \frac{0 \times 0.9 + 1 \times 0.87 + 0 \times 0.83 + 0 \times 0.89 + 0 \times 0.86}{0.9 + 0.87 + 0.83 + 0.89 + 0.86} < 0.5$ . Thus, the sample of the first line cannot be considered as a spike. Considering  $HC(2)$ ,  $HC(4)$ ,  $HC(5)$ ,  $HC(6)$ , or  $HC(8)$  is less than 0.5, 2nd, 4th, 5th, 6th, or 8th lines are not a spike. Also, since  $HC(3)$ ,  $HC(7)$ , or  $HC(9) \geq 0.5$ , 3rd, 7th, or 9th lines can be considered as spikes.

Usually, when a window moves along the signal, there are some peaks higher than a defined threshold named spikes. It is obvious that the amplitudes of the spikes are not alike. As can be seen in Fig. 7d, each of the four potential spikes detected by the method 3 has different amplitude. There is little room for doubt that we should consider each of them separately. To be more precise, the effect of the 2nd potential spike is much more pronounced than for the 3rd or 4th spike.

We also have another proposal to combine some existing methods based on the fuzzy and probability theory. In this method, we consider each answer as a fuzzy number between 0 and 1. Assume Fig. 8 is an output of using a window-based spike detection approach. There is no doubt that for the first peak and the third peak attained by a window-based spike detection method, the probabilities of being the real spikes are 1 and 0.5 respectively.

To generalize the concept, we can define two functions as follows:

$$h_{dp} = 0.5 + \frac{d_p}{2d_{\max}} \quad (5)$$

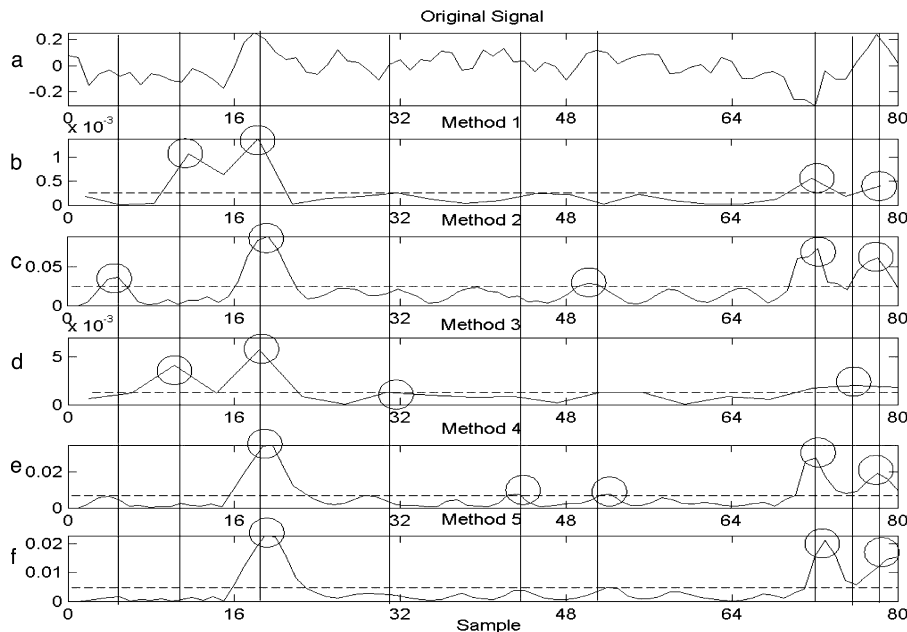


**Fig. 7.** The proposed method for combination four existing methods: (a) original signal, (b) FD with DWT, (c) FD with Savitzky-Golay, (d) SNEO with DWT, (e) standard deviation with DWT, and (f) SNEO with Savitzky-Golay filter.

**Table 1**

Results of these suggested, improved, and existing methods on the realistic synthetic neuronal data.

Method	Parameters	−5 dB	0 dB	5 dB	10 dB	20 dB	50 dB
SNEO <a href="#">Azami and Sanei (2014)</a>	TP	40%	48%	64%	84%	98%	100%
	FN	60%	52%	46%	16%	2%	0%
Improved SNEO by DWT and Hilbert transform	TP	96%	97%	100%	100%	100%	100%
	FN	4%	3%	0%	0%	0%	0%
	FP	47%	30%	0%	0%	0%	0%
Improved SNEO by intelligent SSA, Savitzky–Golay filter and Hilbert transform	TP	95%	97%	100%	100%	100%	100%
	FN	5%	3%	0%	0%	0%	0%
	FP	51%	22%	2%	0%	0%	0%
Improved SNEO by intelligent SSA and Hilbert transform	TP	<b>100%</b>	<b>100%</b>	100%	100%	100%	100%
	FN	<b>0%</b>	<b>0%</b>	0%	0%	0%	0%
	FP	<b>25%</b>	<b>8%</b>	2%	0%	0%	0%
Improved SNEO by EEMD and Hilbert transform	TP	80%	91%	<b>100%</b>	<b>100%</b>	<b>100%</b>	<b>100%</b>
	FN	20%	9%	<b>0%</b>	<b>0%</b>	<b>0%</b>	<b>0%</b>
	FP	78%	39%	<b>0%</b>	<b>0%</b>	<b>0%</b>	<b>0%</b>
Improved SNEO by intelligent KF and Hilbert transform	TP	97%	98%	99%	100%	100%	100%
	FN	3%	2%	1%	0%	0%	0%
	FP	53%	19%	2%	0%	0%	0%
Spike detection using FD, DWT, and Hilbert transform	TP	96%	98%	100%	100%	100%	100%
	FN	4%	2%	2%	0%	0%	0%
	FP	46%	18%	2%	0%	0%	0%
Spike detection using FD, intelligent Savitzky–Golay filter and Hilbert transform	TP	97%	99%	100%	100%	100%	100%
	FN	3%	1%	0%	0%	0%	0%
	FP	69%	40%	39%	25%	32%	25%
Spike detection using FD, intelligent SSA, and Hilbert transform	TP	98%	99%	98%	100%	100%	100%
	FN	2%	1%	2%	0%	0%	0%
	FP	10%	16%	6%	10%	4%	2%
Spike detection using FD, EEMD and Hilbert transform	TP	84%	90%	100%	100%	100%	100%
	FN	16%	10%	0%	0%	0%	0%
	FP	84%	54%	12%	10%	4%	4%
Spike detection using FD, intelligent KF and Hilbert transform	TP	96%	98%	100%	100%	100%	100%
	FN	4%	2%	0%	0%	0%	0%
	FP	61%	41%	41%	30%	25%	22%
Spike detection using standard deviation, DWT, and Hilbert transform	TP	100%	100%	100%	100%	100%	100%
	FN	0%	0%	0%	0%	0%	0%
	FP	40%	20%	10%	14%	15%	11%
Spike detection using standard deviation, intelligent Savitzky–Golay filter, and Hilbert transform	TP	98%	96%	100%	100%	100%	100%
	FN	2%	4%	0%	0%	0%	0%
	FP	64%	26%	30%	13%	18%	16%
Spike detection using standard deviation, intelligent SSA, and Hilbert transform	TP	98%	98%	100%	100%	100%	100%
	FN	2%	2%	0%	0%	0%	0%
	FP	50%	20%	16%	10%	14%	10%
Spike detection using standard deviation EEMD, and Hilbert transform	TP	83%	90%	100%	100%	100%	100%
	FN	17%	10%	0%	0%	0%	0%
	FP	78%	44%	18%	14%	13%	8%
Spike detection using standard deviation, intelligent KF and Hilbert transform	TP	97%	98%	98%	100%	100%	100%
	FN	3%	2%	2%	0%	0%	0%
	FP	61%	24%	25%	16%	17%	14%
NCED <a href="#">Mtetwa and Smith (2006)</a>	TP	96%	94%	96%	98%	98%	98%
	FN	4%	6%	4%	2%	2%	2%
	FP	62%	54%	42%	28%	22%	16%
The first proposed combination method	TP	<b>100%</b>	<b>100%</b>	<b>100%</b>	<b>100%</b>	<b>100%</b>	<b>100%</b>
	FN	<b>0%</b>	<b>0%</b>	<b>0%</b>	<b>0%</b>	<b>0%</b>	<b>0%</b>
	FP	<b>6%</b>	<b>5%</b>	<b>1%</b>	<b>0%</b>	<b>0%</b>	<b>0%</b>
The second proposed combination method	TP	<b>100%</b>	<b>100%</b>	<b>100%</b>	<b>100%</b>	<b>100%</b>	<b>100%</b>
	FN	<b>0%</b>	<b>0%</b>	<b>0%</b>	<b>0%</b>	<b>0%</b>	<b>0%</b>
	FP	<b>6%</b>	<b>4%</b>	<b>0%</b>	<b>0%</b>	<b>0%</b>	<b>0%</b>

Bold values are the best results.

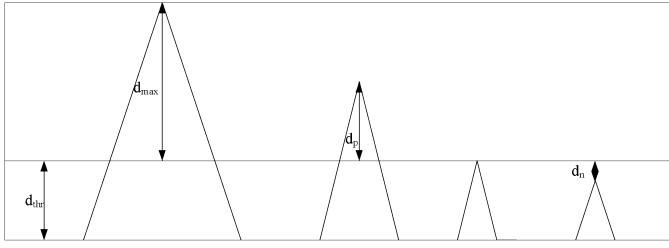


Fig. 8. The output when a window-based spike detection approach is employed.

$$h_{d_n} = 0.5 - \frac{d_n}{2d_{thr}} \quad (6)$$

where  $d_p$  and  $d_n$  are the distance between a defined threshold and a peak upper and under of the threshold respectively and  $h_{d_p}$  and  $h_{d_n}$  respectively are the fuzzy amount for a peak upper and lower than a defined threshold. It is worth noting that when  $d_p = d_{max}$ , then  $h_{d_p} = 1$  as well as if the amplitude of a peak equals with the defined threshold or  $d_p = 0$ , then  $h_{d_p} = 0.5$ .

Using the definition, unlike employing the conventional methods which have 0 and 1 for each peak, we can define much more precise amounts based on the fuzzy theory as follows:

$$HCF = \frac{\lambda_1 SDA_1 h_{d_1} + \lambda_2 SDA_2 h_{d_2} + \dots + \lambda_n SDA_n h_{d_n}}{SDA_1 + SDA_2 + \dots + SDA_n} \quad (7)$$

where  $h_{d_i}$  is  $h_{d_{p_i}}$  or  $h_{d_{n_i}}$  when the peak is respectively higher or lower than the defined threshold. It should be mentioned that this kind of definition is very valuable for combination of a number of spike detection methods. For

$$\text{example, for the second line of Fig. 7, we have: } HCF(2) = \frac{1 \times 0.9 \times \left(0.5 + \frac{0.7}{0.9}\right) + 0 \times 0.87 \times 0 + 1 \times 0.83 \times \left(0.5 + \frac{0.45}{0.9}\right) + 0 \times 0.89 \times 0 + 0 \times 0.86 \times 0}{0.9 + 0.87 + 0.83 + 0.89 + 0.86} < 0.5$$

thus, the sample of the second line cannot be considered as a spike. Like the results of the first method for combination of spike detection approaches, because  $HCF(1)$ ,  $HCF(2)$ ,  $HCF(4)$ ,  $HCF(5)$ ,  $HCF(6)$ , and  $HCF(8)$  are less than 0.5, each of 1st, 2nd, 4th, 5th, 6th, and 8th lines is considered not a spike. However, since  $HC(3)$ ,  $HC(7)$ , or  $HC(9) \geq 0.5$ , 3rd, 7th, or 9th line can be considered a spike. The flow chart of the proposed Approach to do spike detection is illustrated in Fig. 9. Simulation data

#### 2.4. Realistic synthetic neuronal signals

Because of the lack of ground-truth data (i.e., spike timings for each neuron) spike detection methods are often difficult to evaluate. In Smith and Mtetwa (2007), the generation and transmission of intracellular signals from neurons to an extracellular electrode have been modeled and a set of MATLAB functions based on this have been provided. The codes have been used here to generate a set of realistic synthetic neural data. They produce realistic signals from a set of nearby neurons including interference from more distant neurons and Gaussian noise. These data best resemble the output of deep mesio-temporal brain discharges observed at cortical electrodes. The model also includes correlated and uncorrelated spike noises in neuronal data as well as some Gaussian noise, to imitate the effect of thermal and amplifier noise (Smith and Mtetwa, 2007).

By following this synthesizing method, we have randomly generated 70 realistic synthetic neuronal data each including Gaussian noise with SNR = −5, 0, 5, 10, 20 and 50 dBs. For each SNR

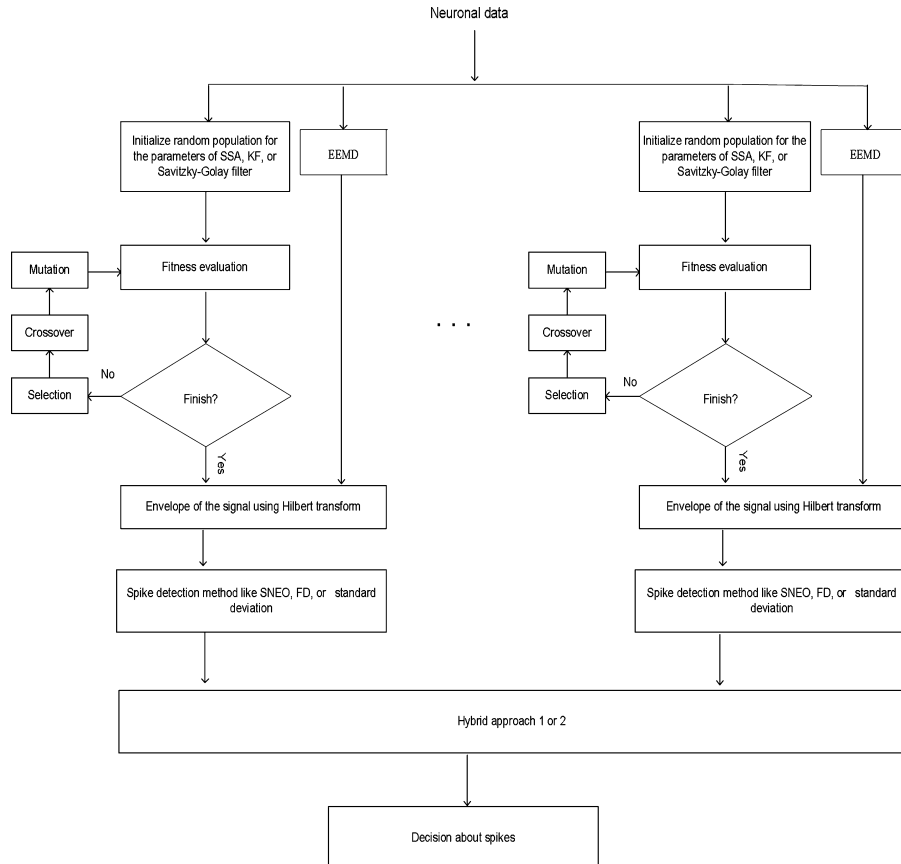


Fig. 9. Flowchart of the proposed approach.



**Table 2**

Comparison of spike detection rates for two best proposed methods, the proposed combination approaches, the two best algorithm proposed in Azami and Sanei (2014) and NCED method (Mtetwa and Smith, 2006) as one of the best spike detection methods tested in real neuronal data.

Method	TP	FN	FP
Spike detection using FD and SSA Azami and Sanei (2014)	94%	6%	17%
Spike detection using FD and SSA method Azami and Sanei (2014)	91%	9%	12%
NCED Mtetwa and Smith (2006)	89%	11%	21%
The first proposed combination method	97%	3%	8%
The second proposed combination method	97%	3%	7%

level, each data contains 12–14 spikes. Therefore, we have about  $70 \times 6 \times 13 = 5460$  spikes to test. One of 70 signals that contains 13 spikes with SNR = 5 dB, randomly selected, shown in Fig. 5.

### 2.5. Real neuronal signal

In addition to a set of realistic synthetic neural data, we evaluated the proposed and existing approaches for the real neuronal signals. The data is a part of a real signal of the CARMEN project managed by Prof. Leslie S. Smith (CARMEN, 2014). It is approximately 900 s long and 20,000 Hz.

## 3. Simulation results

Three different parameters, including the true positive (TP) miss or false negative (FN) and false positive (FP) ratios were used to evaluate the performance and effectiveness of the proposed methods. TP and FP were introduced in Section 2 and  $FN = (N_m/N)$ , where  $N_m$  shows the number of missed detected spikes.

In Table 1, all of the spike detection approaches, which have been proposed in Azami and Sanei (2014), improved by Hilbert transform and intelligent filter for the semi-real data are shown. In addition, we replace the EMD with EEMD. By comparison between the results in this table and Table 1 in Azami and Sanei (2014), it can be observed that the majority of results are slightly increased by about 1–3% in comparison with Table 1 in Azami and Sanei (2014).

As can be seen in Table 1, the performance of KF is similar to Savitzky–Golay filter. The results demonstrate that DWT has better performance than Savitzky–Golay filter and both of them can achieve considerably better spike detection than SNEO. As can be observed in Table 1, when SNRs > 0, improved SNEO by EEMD and Hilbert transform performs best in terms of all the parameters. In contrast, when SNRs < 0, SNEO with Hilbert transform and intelligent SSA is the best approach with regard to TPs and FNs not only among SNEO-based methods but also among all the proposed methods. The best method using standard deviation regarding to TPs and FNs is achieved using DWT.

Moreover, the final rows of the table contain NCED as the best algorithm in Mtetwa and Smith (2006), and the proposed hybrid approaches. As it can be observed, the two combination approaches enhance the existing accuracies largely, with the second hybrid approach is slightly better than the first one.

After assessing the proposed and conventional methods on realistic synthetic neural data, these methods were evaluated using real neuronal signals. In Table 2 the two best algorithms proposed in Azami and Sanei (2014), namely improved SNEO by SSA and spike detection using FD and SSA, NCED (the best algorithm proposed in Mtetwa and Smith (2006)) and the two proposed hybrid approaches in this study are compared using the real neuronal data. Like the realistic synthetic neuronal data, for the real neuronal data, the two hybrid approaches are superior with regard to all the three parameters TP, FN and FP to the aforementioned existing methods, even though the second hybrid algorithm performs slightly better than the first one. These methods are superior to NCED as the best

method among various approaches suggested in Mtetwa and Smith (2006).

## 4. Conclusions

The aim of the piece of research is to investigate and illustrate the capability of the intelligent filtering approaches, and two novel hybrids ensemble methods to detect the extracellular neuronal data. In many of conventional noise reduction algorithms, such as SSA, there are several parameters that must be adjusted using many trials. We have proposed using an intelligent approach to adjust the SSA and KF, and employing the residual signal obtained by EEMD. It is worth mentioning that the novel intelligent filter reduces the effect of noise and it can be used in many other applications. In addition, we took the Hilbert transform of the neuronal data to turn the negative spikes into positive ones and, consequently, increase the accuracy of almost every existing spike detector. Finally, in order to boost the performance of the conventional approaches, we have proposed two novel and influential techniques based on combination of the conventional spike detection methods. The results indicate superiority of the proposed methodology.

Future research works will seek to improve our methods by using a number of approaches based on data fusion, combination or ensemble concepts used in classification and clustering to combine some existing spike detection methods. Spike sorting can also be considered as another step to follow after spike detection in the future.

## Acknowledgements

The authors wish to thank Prof. Leslie S. Smith who gave real neuronal data. The authors also are grateful to Prof. Leslie S. Smith and Morteza Saraf for their valuable comments.

## References

- Azami H, Sanei S. Automatic signal segmentation based on singular spectrum analysis and imperialist competitive algorithm. In: 2nd International e-Conference on Computer and Knowledge Engineering, IEEE Xplore; 2012. p. 50–5.
- Azami H, Sanei S. An evaluation of spike detection approaches for noisy neuronal data; assessment and comparison. *Neurocomputing* 2014;133:491–506.
- Azami H, Sanei S, Mohammadi K, Hassanpour H. A hybrid evolutionary approach to segmentation of non-stationary signals. *Digital Signal Process* 2013;23(4):1103–14.
- Azami H, Hassanpour H, Escudero J, Sanei S. An evolutionary segmentation approach for non-stationary signals. *J Adv Res* 2014. <http://dx.doi.org/10.1016/j.jare.2014.03.004>.
- Benitez D, Gaydecki PA, Zaidi A, Fitzpatrick AP. The use of the Hilbert transform in ECG signal analysis. *Comput Biol Med* 2001;31(5):399–406.
- CARMEN. <http://www.carmen.org.uk/>; 2014.
- Kim S, McNames J. Automatic spike detection based on adaptive template matching for extracellular neural recordings. *J Neurosci Methods* 2007;165(2):165–74.
- Lin S, Li P. Automatic contrast enhancement using ensemble empirical mode decomposition. *IEEE Trans Ultrason Ferroelectr Freq Control* 2011;58(12):2680–8.
- Liu X, Yang X, Zheng N. Automatic extracellular spike detection with piecewise optimal morphological filter. *Neurocomputing* 2012;79:132–9.
- Lue J, Ying K, Bai J. Savitzky–Golay smoothing and differentiation filter for even number data. *Signal Process* 2005;85(7):1429–34.
- Maccione A, Gandolfi M, Massobrio P, Novellinoc A, Martinoiab S, Chiappalone M. A novel algorithm for precise identification of spikes in extracellularly recorded neuronal signals. *J Neurosci Methods* 2009;177(1):241–9.

- Mandic DP, Rehman N, Wu Z, Huang NE. Empirical mode decomposition-based time-frequency analysis of multivariate signals: the power of adaptive data analysis. *Signal Process Mag IEEE* 2013;30(6):74–86.
- Martinez J, Pedreira C, Ison MJ, Quiroga RQ. Realistic simulation of extracellular recordings. *J Neurosci Methods* 2009;184(2):285–9.
- Mtewa N, Smith LS. Smoothing and thresholding in neuronal spike detection. *Neurocomputing* 2006;69(10–12):1366–70.
- Nenadic Z, Burdick JW. Spike detection using the continuous wavelet transform. *IEEE Trans Biomed Eng* 2005;52(1):74–87.
- Procházka A, Vyšata O, Ťupa O, Yadollahi M, Vališ M. Discrimination of axonal neuropathy using sensitivity and specificity statistical measures. *Neural Comput Appl* 2014., <http://dx.doi.org/10.1007/s00521-014-1622-0>.
- Quiroga RQ. What is the real shape of extracellular spikes? *J Neurosci Methods* 2009;177(1):194–8.
- Sanei S, Lee TKM, Abolghasemi V. A new adaptive line enhancer based on singular spectrum analysis. *IEEE Trans Biomed Eng* 2012;59(2).
- Savitzky A, Golay MJ. Smoothing and differentiation of data by simplified least square procedure. *Anal Chem* 1964;36(8):1627–39.
- Shahid S, Walker J, Smith LS. A new spike detection algorithm for extracellular neural recordings. *IEEE Trans Biomed Eng* 2010;57(4):853–66.
- Smith LS, Mtewa N. A tool for synthesizing spike trains with realistic interference. *J Neurosci Methods* 2007;159(1):170–80.
- Smith LS, et al. The CARMEN e-Science pilot project: neuroinformatics work packages. In: *Proceedings of the UK e-Science All Hands Meeting*; 2007.
- Takekawa T, Ota K, Murayama M, Fukai T. Spike detection from noisy neural data in linear-probe recordings. *Eur J Neurosci* 2014;39(11):1943–50.
- Thrane N, Wismer J, Konstantin-Hansen H, Gade S. Application note: practical use of the Hilbert transform. Denmark: Brüel&Kjær; 1995.
- Yang X, Shamma SA. A totally automated system for the detection and classification of neural spikes. *IEEE Trans Biomed Eng* 1988;35(10):806–16.